STORM TRACK CHARACTERIZATION BASED ON REANALYSIS DATA

BSC-ESS-2016-005

Raül Marcos - Nube González-Reviriego –
Francisco J. Doblas-Reyes

Earth Sciences Department
Barcelona Supercomputing Center - Centro Nacional de Supercomputación (BSC-CNS)

25 November 2016

TECHNICAL REPORT

Series: Earth Sciences (ES) Technical Report

A full list of ES Publications can be found on our website under:

http://www.bsc.es/projects/earthscience/ES-CFU/doku.php?id=start

Barcelona Supercomputing Center–Centro Nacional de Supercomputación (BSC-CN)

C/Jordi Girona, 31 | 08034 Barcelona (Spain)

Summary

In this report we characterized global storm tracks from the ERA-Interim and JRA-55 standard deviation of daily sea level pressure (SLP) anomalies for the period 1981-2015 using a 2-10 day band-pass filter. At this synoptic time-scale both reanalyses showed similar storm track patterns. Slight differences were detected regarding the magnitude of the variability in scattered areas. In the Northern Hemisphere they successfully marked the maxima in the western ocean regions. In the austral hemisphere the circumpolar storm track was also well identified. Regarding the reduced variability area in the inter-tropical belt, it was well detected in both reanalysis.

Contents

Index of figures

1. Introduction

The term storm track is used to describe the main paths followed by tropical and extra-tropical cyclones in both hemispheres. These *routes* are more prevalent over the oceans due to the smaller surface roughness. In fact, without orographic obstacles this kind of systems maintain their structure during more time than inland and, thus, they can travel further without changing their trajectory (Hoskins & Hodges 2002).

In the boreal extra-tropics these routes begin in the western part of the oceans, where the cyclones form, and tend to dissipate in the eastern shores, when entering land (Chang et al. 2002). In the austral extra-tropics, on the other hand, the existence of a continuous ocean surrounding Antarctica facilitates the existence of a well-defined circumpolar storm track (e.g. Mendes et al. 2003). Finally, the inter-tropical cyclones tend to form in the eastern part of the oceans (even within land in Africa), dissipating either in the western shores or in the northern/southern extra-tropical storm tracks (e.g. Hopsch et al. 2007). These systems, however, are fewer than their extra-tropical counterparts and with characteristic time-scales that vary greatly among them (e.g. Peng et al. 2012).

The storm track patterns can be modified through alterations in the atmospheric general circulation induced by remote events such *El Niño Southern Oscillation* or global warming (Bengtsson et al. 2006; Ashok et al. 2007). The disturbances on the storm tracks driven by these phenomena range from weather to climatic scales and can have significant impacts in our economy and society. In the field of wind-power production anomalies in the storm tracks can dramatically reduce power generation (Yin 2005; Liu et al. 2008). For instance, facilities in wind-prone regions could lose their capacity if the storms fuelling their specific wind regimes do not travel across the area in the usual way. The opposite case is hard to find because no facilities are placed in low-wind climatic regions.

From the seasonal and sub-seasonal perspective, the possibility to foretell variations in wind regimes with months/weeks in advance could be of great interest for stakeholder short-to-midterm planning. The characterization of storm track hot-spots helps to achieve this objective by locating the most interesting areas to focus the research efforts on. Storm track identification can be achieved through different techniques based either on the so-called *Lagrangian* or *Eulerian* frameworks (e.g. Hoskins & Hodges 2002).

The *Lagrangian* concept seeks to identify each individual pressure system and follows its evolution in time to obtain the statistical trajectory distribution (e.g. Klein 1957). The *Eulerian* approach, on the other hand, is focused on the study of statistic variability parameters on a set of grid points to issue maps of the preferred traveling zones (e.g. Blackmon 1976; Blackmon et al. 1977). Although both methodologies have advantages and disadvantages, the *Eulerian* approximation is preferred in RESILIENCE because it can provide global storm track maps in a seamless and straightforward way.

2. Data and methodology

The global synoptic storm tracks have been characterized from a *Eulerian* perspective computing the standard deviation of daily sea level pressure (SLP) anomalies (averaged from 6-hourly values) from the ERA-Interim and JRA-55 reanalysis (Doblas-Reyes & Déqué 1998) filtered using a 2-10 day band-pass filter over a 35-year period (1981-2015). Another possible option could have been to use the 6-hourly values instead of their daily aggregation. In that case we would have achieved a finer resolution in the storm tracks but at a higher computational cost.

2.1. Data

We have used global daily SLP data for the period 1981-2015 from ERA-Interim and JRA-55 reanalysis. The resolution for ERA-Interim is 0.75º (~80km) whereas for JRA-55 is 1.25º (~140km). The daily time series come from the aggregation of the original 6-hourly files.

2.1.1. ERA-Interim

The ERA-Interim reanalysis dataset (Dee et al. 2011) is the latest global atmospheric reanalysis issued by the European Centre for Medium-Range Weather Forecasts (ECMWF). It spans from 1979 to present and updated in a real-time basis. In comparison to the previous system, ERA-40 (Uppala et al. 2005), it shows multiple improvements such as the incorporation of the four-dimension variational data assimilation approach (4D-Var), the increase of model resolution or the enhancement of the forecast model physics.

2.1.2. JRA-55

The JRA-55 reanalysis dataset (Kobayashi et al. 2015) is the second global atmospheric reanalysis supplied by the Japan Meteorological Agency (JMA). It covers the period from 1958 to present and is also updated in real-time. It is the first global reanalysis that applies the four-dimensional variational analysis for the last half-century. Besides using the 4D-Var method, it improves the previous reanalysis, JRA-25 (Onogi et al. 2007), by including variational bias correction (VarBC) for satellite radiances, a new radiation scheme or the introduction of dynamic greenhouse gas concentrations.

2.2. Methodology

The Eulerian storm track diagnosis has been approached by computing the standard deviation of daily SLP anomalies at every grid point in a frequency band associated with synoptic time-scales (2-10 days). The storm tracks have been obtained with the ERA-Interim and JRA-55 reanalysis to reach robust conclusions about the patterns identified. Firstly, we had to select the variable to characterize the storm tracks. We have chosen SLP because they are less influenced by the global warming signal compared to geopotential height (Gillett et al. 2013). Secondly, we have set a characteristic time-scale between 2 and 10 days to retain extra-tropical cyclone variability. Hence, as a final step we have filtered out the events with frequencies higher or lower than these thresholds (**Figure 1**).

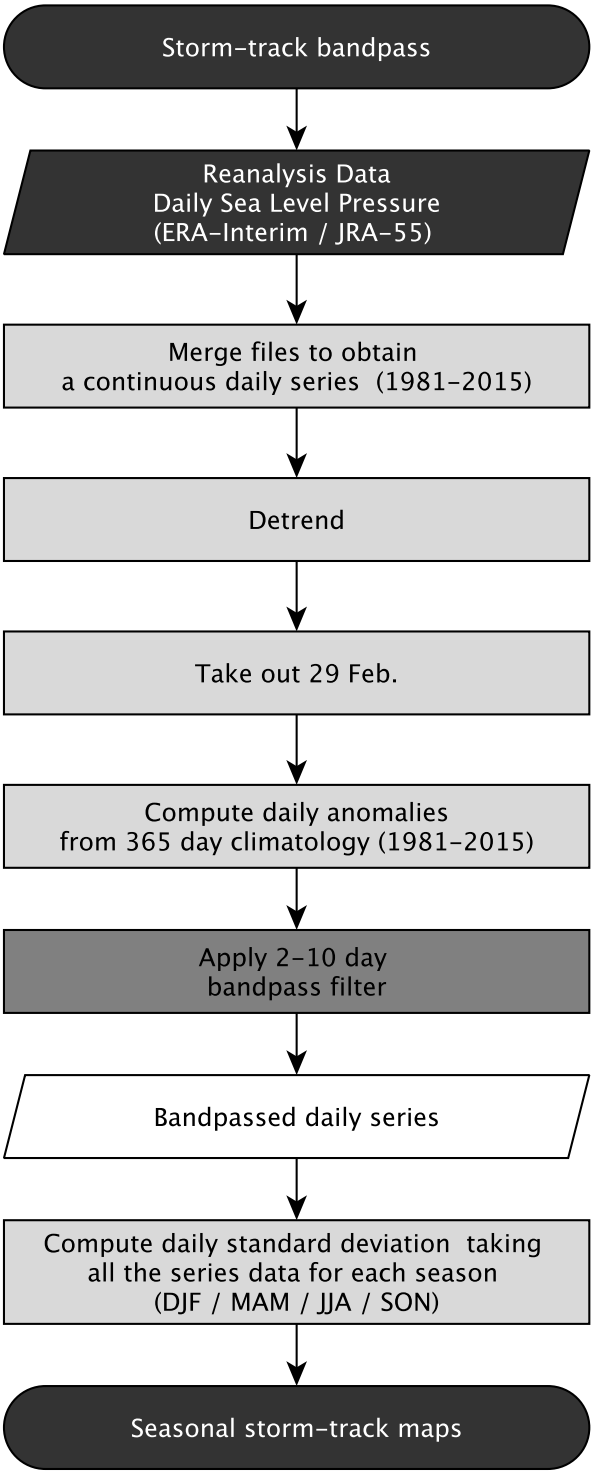

Figure 1. *Work-flow diagram*

Work-flow diagram for the computation of seasonal storm tracks. Daily anomalies of sea level pressure data are computed for each grid point and a 2-10 band-pass filter applied. The corresponding standard deviation is then calculated before plotting the results.

3. Results

Figure 2 and Figure 3 show the results of filtering the SLP anomalies of ERA-Interim and JRA-55, respectively, through a 2-to-10 day band-filter for each season. Both reanalyses agree on the identification of two extra-tropical storm tracks, one in each hemisphere. They also show the belt of low variability in the inter-tropical region. Thus, these two reanalyses are in high agreement with each other and, as expected, they are in accordance with the results of previous studies (e.g. Chang et al. 2002; Hoskins & Hodges 2002; Mendes et al. 2003). The slight differences observed are more related with the magnitude of the variability rather than with its geographical location.

At the 2-10 day synoptic time-scale the inter-tropical pattern is characterized by lower variability in all seasons in comparison to the extra-tropical areas. This is a consequence of the dominant structures in this area, the Intertropical Convergence Zone (ITCZ) and the high pressure belts (e.g. Schneider 2006). In fact, their specific frequencies fall out the range of the filter (Blackmon & Lee 1984), and though the tropical cyclones could be within the band retained by the filter, they are not as recurrent as their extra-tropical counterparts. So, the contribution to the variability is rather limited.

In the northern extra-tropics, on the other hand, there are two high-variability regions that can be found in eastern North America and central north Pacific, where most storm systems form (e.g. Schneider 2006). These storm tracks are more intense in DJF (December-January-February), followed by SON (September-October-November) and MAM (March-April-May). In JJA (June-July-August) their activity is weaker and almost disappears. This behaviour is the consequence of the baroclinic instability combined with the specific distribution of continents and oceans, which determines the spatio-temporal distribution of the variability observed (e.g. Chang et al. 2002).

In the southern hemisphere there is a continuous extra-tropical storm-track pattern surrounding Antarctica, which is more intense in JJA and weaker in DJF. In MAM and SON, although the storm track is not as strong as in JJA, it is stronger than its counterpart in the northern hemisphere. This is due to the continuous ocean surrounding the continent, which stabilizes and strengthens the circulation (e.g. Chang et al. 2002; Schneider 2006). This particular configuration has specific implications for Antarctica's weather and climate. Therefore, it is an object of intense research.

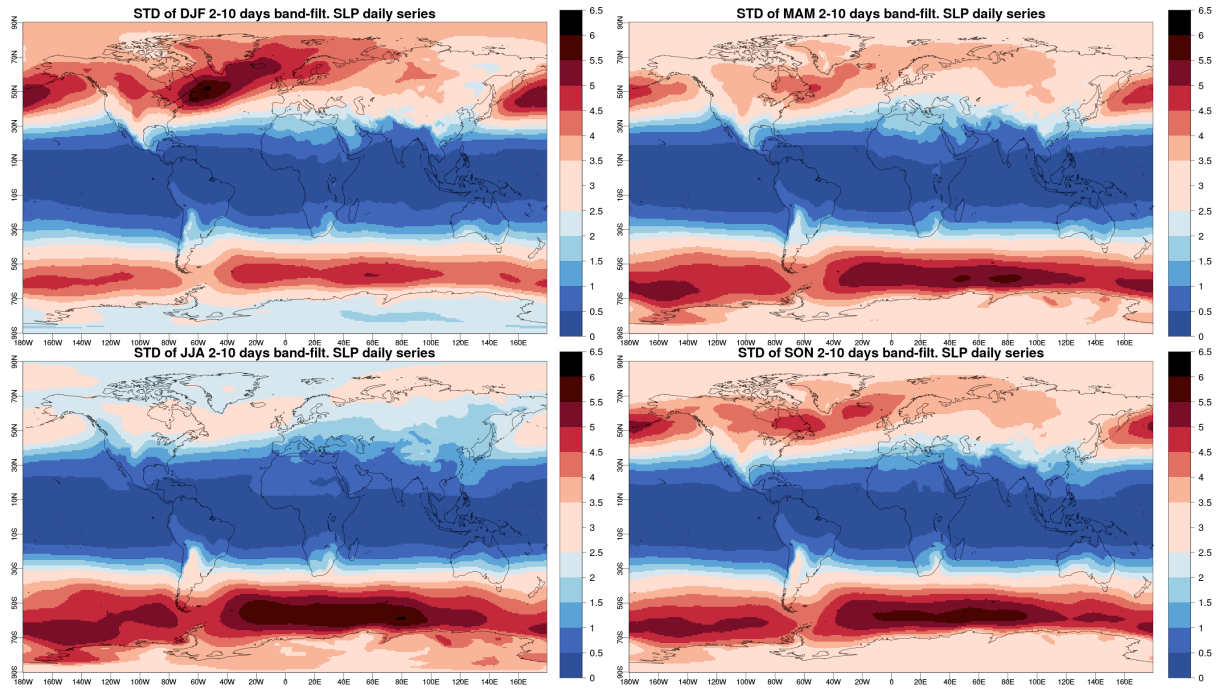

Figure 2. *Standard deviation of the 2-to-10 day bandpass filtered ERA-Interm data.*

Standard deviation of the 2-to-10 day bandpass filtered ERA-Interim data. Daily SLP time series have been detrended for each season over 1981-2015.

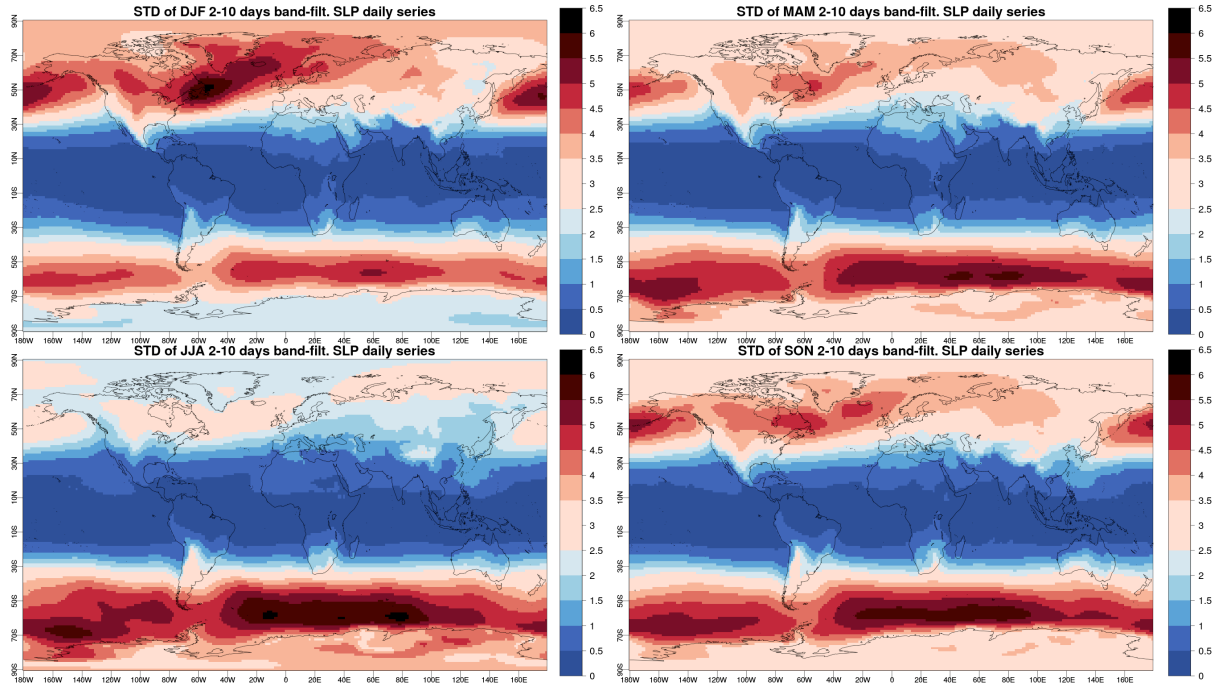

Figure 3. As in Figure 2, but for the JRA-55 reanalysis.

4. Conclusions

In this study, we have characterized the synoptic storm tracks from a *Eulerian* perspective computing the standard deviation of daily SLP anomalies from the ERA-Interim and JRA-55 reanalyses filtered with a 2-10 day band-pass filter applied on the 35-year period 1981-2015.

We have identified the boreal and austral extra-tropical storm paths and the inter-tropical low variability area. We have also located the geographical regions where the activity is more prevalent along with the corresponding intensity of the annual cycle. In fact, the results of both reanalyses are highly concordant with the existing literature in the field (e.g. Chang et al. 2002; Hoskins & Hodges 2002; Mendes et al. 2003). The differences between both datasets are small and mainly related to the magnitude of the variability obtained in particular regions. Nevertheless, the similarity between both outcomes is remarkable. So, this gives us a robust characterization of the storm tracks portrayed.

The general idea behind our strategy has been to characterize storm-tracks with ERA-Interim and JRA-55 reanalysis and, hence, locate regions of interest for wind-power forecasting. In fact, looking at the seasonal 10-metre wind speed climatology and variability maps from ERA-Interim (**Figure 4** and **Figure 5**), we can see that the SLP storm tracks coincide with the areas of maximum average wind speed and high wind speed variability. Additionally, taking into account that the Japanese reanalysis is a recent tool that still has not been widely used in studies of this kind, this work shows the JRA-55 reanalysis provides similar results to the well-established ERA-Interim reanalysis.

This diagnostic work is part of the studies aimed to characterize the variability of wind speed in the RESILIENCE project. Thus, in this framework it is a first step that helps to locate the hot-spot regions for the study of seasonal/sub-seasonal wind forecasts. Further research on this topic will be focused on the characterization of the 10-metre wind statistical distribution and the weather regimes impact on wind speed.

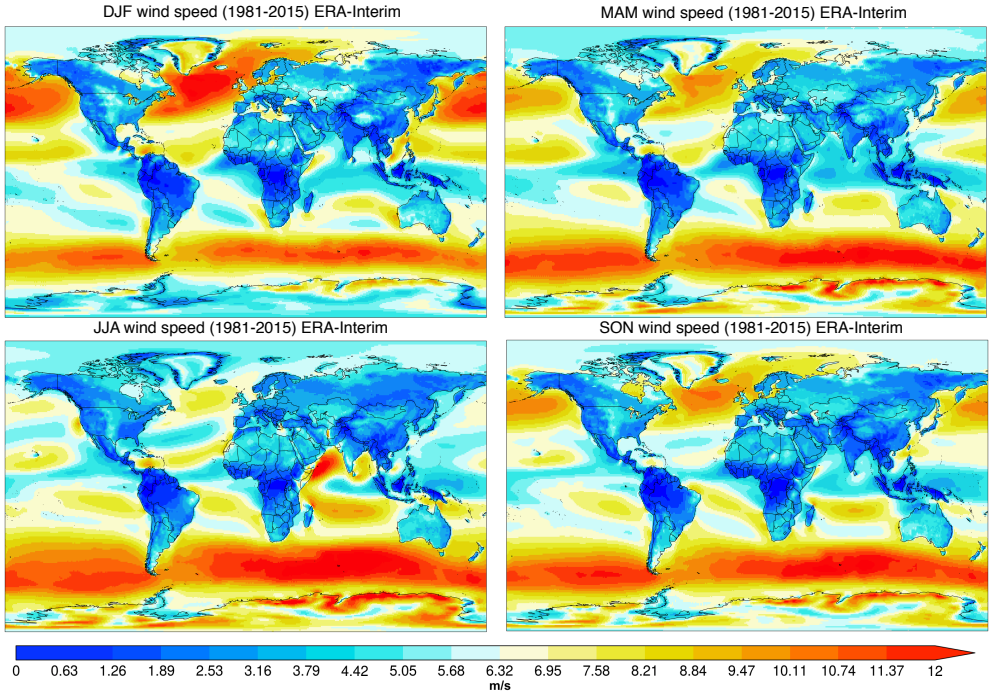

Figure 4. *Intra-seasonal climatology of the ERA-Interim mean 10-metre wind*

Intra-seasonal climatology of the ERA-Interim mean 10-metre wind computed from the period 1981-2015.

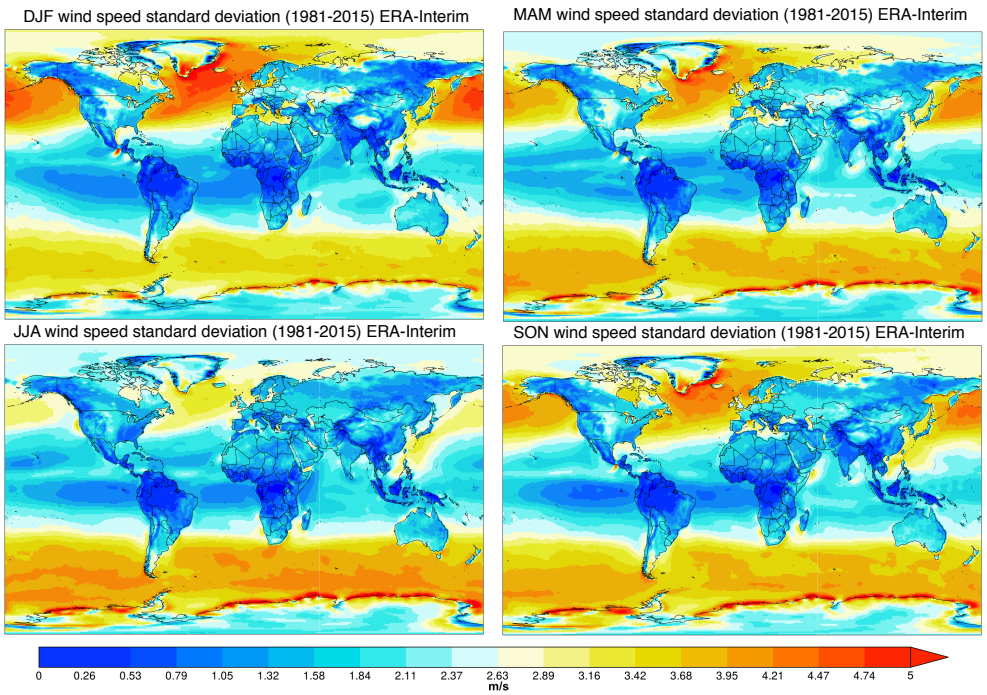

Figure 5. *Intra-seasonal standard deviation of the ERA-Interim 10-metre wind*

Intra-seasonal standard deviation of the ERA-Interim 10-metre wind computed for the period 1981-2015.

5. Acknowledgements

We thank the RESILIENCE project funding (CGL2013-41055-R) for allowing us to carry out this research. We acknowledge the ECMWF for the ECMWF System 4 ensemble re-forecast data and the ERA-Interim reanalysis. We also acknowledge the JMA for the use of the JRA-55 reanalysis dataset.

6. References

Ashok, K., Nakamura, H. & Yamagata, T., 2007. Impacts of ENSO and Indian Ocean dipole events on the Southern Hemisphere storm track activity during austral winter. In *Journal of Climate*. pp. 3147–3163.

Bengtsson, L., Hodges, K.I. & Roeckner, E., 2006. Storm tracks and climate change. *Journal of Climate*, 19(15), pp.3518–3543.

Blackmon, M. & Lee, Y.-H., 1984. Horizontal structure of 500mb heigth fluctuations with long, intermediate and short time-scales. *Journal of the Atmospheric Sciences*, 41(6), pp.961–979.

Blackmon, M.L., 1976. A Climatological Spectral Study of the 500 mb Geopotential Height of the Northern Hemisphere. *Journal of the Atmospheric Sciences*, 33(8), pp.1607–1623.

Blackmon, M.L. et al., 1977. An Observational Study of the Northern Hemisphere Wintertime Circulation. *Journal of the Atmospheric Sciences*, 34(7), pp.1040–1053.

Chang, E.K.M., Lee, S. & Swanson, K.L., 2002. Storm track dynamics. *Journal of Climate*, 15(16), pp.2163–2183.

Dee, D.P. et al., 2011. The ERA-Interim reanalysis: Configuration and performance of the data assimilation system. *Quarterly Journal of the Royal Meteorological Society*, 137, pp.553–597.

Doblas-Reyes, F.J. & Déqué, M., 1998. A Flexible Bandpass Filter Design Procedure Applied to Midlatitude Intraseasonal Variability. *Monthly Weather Review*, 126(12), pp.3326–3335.

Gillett, N.P., Fyfe, J.C. & Parker, D.E., 2013. Attribution of observed sea level pressure trends to greenhouse gas, aerosol, and ozone changes. *Geophysical Research Letters*, 40(10), pp.2302–2306.

Hopsch, S.B. et al., 2007. West African storm tracks and their relationship to Atlantic tropical cyclones. *Journal of Climate*, 20(11), pp.2468–2483.

Hoskins, B.J. & Hodges, K.I., 2002. New Perspectives on the Northern Hemisphere Winter Storm Tracks. *Journal of the Atmospheric Sciences*, 59(6), pp.1041–1061.

Klein, W.H., 1957. *Principal tracks and mean frequencies of cyclones and anticyclones in the Northern Hemisphere*,

Kobayashi, S. et al., 2015. The JRA-55 Reanalysis: General Specifications and Basic Characteristics. *Journal of the Meteorological Society of Japan.*, 93(1), pp.5–48.

Liu, W.T., Tang, W. & Xie, X., 2008. Wind power distribution over the ocean. *Geophysical Research Letters*, 35(13).

Mendes, D., Trigo, I. & Miranda, P., 2003. South Hemisphere circulation regime and storm

track variability. *Geophysical Research*, 5.

Onogi, K. et al., 2007. The JRA-25 Reanalysis. *Journal of the Meteorological Society of Japan*, 85(3), pp.369–432.

Peng, M.S. et al., 2012. Developing versus Nondeveloping Disturbances for Tropical Cyclone Formation. Part I: North Atlantic*. *Monthly Weather Review*, 140(4), pp.1047–1066.

Schneider, T., 2006. The general circulation of the atmosphere. *Annual Review of Earth and Planetary Science*, 34(1), pp.655–688.

Uppala, S.M. et al., 2005. The ERA-40 re-analysis. *Quarterly Journal of the Royal Meteorological Society*, 131(612), pp.2961–3012.

Yin, J.H., 2005. A consistent poleward shift of the storm tracks in simulations of 21st century climate. *Geophysical Research Letters*, 32(18), pp.1–4.

7. Annex

The scripts used to filter the data are based on *cdo* instructions and are written in *bash*. They are placed in the folder *https://earth.bsc.es/gitlab/es/ESS/tree/master/stormtracks/Bash* under these names:

- bandpass_ERAint.sh
- bandpass_JRA.sh

There are a couple of other scripts that launch them in *amdahl* and *moore*, defining the main characteristics of the respective runs. They are:

- bandpass_eraint_job.sh
- bandpass_jra_job.sh

Afterwards, the results obtained are plotted with the R script,

- storm_track_readplot. R

Inside *bandpass_ERAint.sh* and *bandpass_JRA.sh* the order of the operations is determined by the requirements of the *cdo bandpass* command. We start by defining the period of study and the minimum and maximum frequencies of the band that we want to compute (*fmin* and *fmax*). The command *cdo bandpass* works with a defined year of 365 days and, consequently, all frequencies given as parameters are interpreted also per year and have to be introduced accordingly. More specifically, since we want a band between 2 and 10 days, we have to establish a minimum 'frequency' of 36.5 (365/10) and a maximum of '182.5' (365/2).

Afterwards the first step is to merge all the files for the required period. This is a two-phase process where the initial stage corresponds to a year-by-year aggregation and the second, to a global unification through *cdo mergetime*. Secondly, we detrend the series with *cdo detrend* just in case any linear trend exists in the dataset. After, we take out each 29 of February with *cdo del29feb* because *cdo bandpass* can only work with years of 365 days. Next we compute the anomaly series through the concatenation of a couple of cdo instructions: *cdo ydaysub* and *cdo ydaymean*. The first one subtracts from each of its members the following element, which is the daily mean in this case. We have to bear in mind that we have to work with the appropriate file type, in this case with the option *-b F32*.

Finally, it is the moment to compute the filtering with *fmin* and *fmax*. We start by applying *cdo bandpass* to the pre-processed complete data. Then, we compute the standard deviation with *cdo timstd* and the seasonal counterparts with *cdo selseas* and *cdo* timstd.